A Generalized PyTheus Quantum Network Interpreter: Automated Analysis and Visualization of Optimized Quantum Architectures

Research Team
Quantum Information Laboratory

July 8, 2025

Abstract

We present a generalized interpreter for PyTheus-optimized quantum networks that automatically analyzes and visualizes complex quantum architectures discovered through automated optimization. The interpreter addresses the critical challenge of understanding machine-designed quantum networks by providing robust algorithms for functional role identification, graph-theoretical analysis, and physically meaningful visualization. Our interpreter accepts both file-based and in-memory network representations, automatically identifies sources, detectors, beam splitters, and ancillas, and generates coordinated native graph plots and optical table representations. Applied to a five-node quantum communication network, the interpreter reveals asymmetric source placement and dual-role node functionality that would be difficult to identify manually. The interpreter successfully handles complex connectivity patterns, avoids visualization artifacts, and provides validation mechanisms for architectural consistency. Our primary contribution is the development of robust interpretation algorithms that can analyze arbitrary PyTheus-generated quantum networks, enabling better understanding of automated quantum architecture design.

1 Introduction

The automated design of quantum networks has emerged as a critical capability for developing large-scale quantum communication and computing systems. Tools like the PyTheus quantum optimization framework (1) can discover complex network architectures that maximize performance objectives, often identifying non-intuitive designs that outperform human-designed alternatives. However, a significant challenge in automated quantum network design is the interpretation and validation of machine-generated architectures.

PyTheus and similar optimization frameworks typically output abstract graph representations with numerical edge weights and vertex configurations. While these representations fully specify the quantum network, they can be difficult for researchers to understand, validate, and translate into physical implementations. The complexity of interpreting these outputs increases dramatically with network size and the sophistication of discovered architectures.

This interpretation challenge has several important consequences: (1) researchers may miss key insights about discovered architectures, (2) validation of optimization results becomes difficult without manual analysis, (3) translation to experimental implementations requires extensive expert interpretation, and (4) comparison between different optimized designs lacks systematic approaches.

In this work, we address these challenges by developing a generalized interpreter for PyTheus quantum network outputs. Our interpreter provides automated analysis capabilities that extract meaningful architectural insights from raw optimization results. The interpreter is designed to handle arbitrary network configurations and scales robustly to networks of varying size and complexity.

The primary contributions of this work are:

1. A robust interpreter architecture for analyzing PyTheus quantum network outputs
2. Automated algorithms for functional role identification (sources, detectors, beam splitters, ancillas)
3. Coordinated visualization capabilities producing both graph-theoretical and optical table representations
4. Validation mechanisms ensuring architectural consistency and identifying potential issues
5. Demonstration of interpreter capabilities on a complex five-node quantum communication network

2 PyTheus Network Interpreter Architecture

2.1 Core Design Philosophy

Our generalized PyTheus interpreter embodies a fundamentally different approach to quantum network analysis. Rather than implementing predefined network categories or hardcoded assumptions about quantum architectures, the interpreter employs adaptive algorithms that analyze any PyTheus-generated graph structure and dynamically infer the underlying quantum network design.

The interpreter's core philosophy centers on three principles: (1) **Complete Generality** – no assumptions about network types, target states, or implementation platforms; (2) **Structure-Driven Analysis** – functional roles emerge from graph topology and configuration data rather than predetermined categories; and (3) **Coordinated Visualization** – mathematical graph representations and physical optical layouts maintain strict consistency.

2.2 Multi-Modal Input Processing

The interpreter features robust input handling that accepts both file-based and in-memory data structures. The `GeneralQuantumNetworkInterpreter` class can process PyTheus configurations and graphs from JSON files, Python dictionaries, or mixed input modes. This flexibility enables integration into automated optimization workflows while supporting interactive analysis.

The input processing system automatically detects data formats and extracts essential network information including vertex sets, edge connectivity patterns, coupling weights, and quantum state specifications. Edge data is parsed from PyTheus's tuple format `(v1, v2, mode1, mode2)` to extract both connectivity and optical mode information.

2.3 Adaptive Structural Analysis

The interpreter's structural analysis pipeline operates through five integrated modules:

Graph Topology Analysis: Computation of vertex degrees, connectivity patterns, and network motifs using NetworkX algorithms. The system calculates betweenness centrality, closeness centrality, and clustering coefficients to identify structural roles.

Functional Role Identification: A hybrid approach that prioritizes configuration-specified roles (such as single emitters) while falling back to structural heuristics. The algorithm analyzes degree distributions, centrality measures, and connectivity patterns to classify vertices as sources, detectors, beam splitters, or ancillas.

Mode Analysis: Examination of optical mode patterns in the edge data to determine implementation strategies. The system identifies mode correlations, wavelength requirements, and coupling schemes.

Implementation Strategy Determination: Integration of structural and mode analysis to recommend optical implementation approaches. The algorithm determines whether networks require single-photon sources, SPDC sources, or other photon generation schemes.

Quantum State Analysis: Analysis of target state structures to validate consistency between network architecture and quantum state requirements. The system extracts photon number distributions, correlation patterns, and basis state structures.

2.4 Visualization Generation Pipeline

The interpreter employs a sophisticated dual-visualization approach that generates both native graph plots and optical table representations from the same underlying analysis.

Native Graph Visualization: The `plot_native_graph` method recreates PyTheus's exact visual style including circular vertex layouts, color-coded edges, and adaptive thickness scaling. The system preserves PyTheus's edge coloring scheme where mode indices map to standard colors (dodgerblue, firebrick, limegreen, etc.) and edge thickness reflects coupling strength.

Optical Table Generation: The `plot_optical_table_setup` method translates abstract graph structures into physically meaningful optical layouts. The system positions sources, beam splitters, and detectors based on signal flow analysis and draws optical connections that correspond directly to graph edges.

The optical table generator includes specialized sub-methods for different implementation schemes: `_plot_single_photon_optical_table` for single-photon networks, `_plot_general_spdc_optical_tabl` for SPDC-based architectures, and adaptive routing algorithms that avoid visualization artifacts.

2.5 Validation and Consistency Mechanisms

The interpreter incorporates comprehensive validation systems to ensure reliability and accuracy. The `_analyze_connectivity` method validates graph consistency and identifies potential structural issues. Edge weight validation ensures that coupling strengths remain within physical bounds.

The visualization pipeline includes artifact prevention mechanisms that ensure all optical elements have proper connectivity. The system validates that the number of identified sources can generate required photon numbers for target states and verifies that detector configurations support the specified measurement schemes.

2.6 API Design and Integration

The interpreter provides both object-oriented and functional interfaces. The main `GeneralQuantumNetworkInt` class offers fine-grained control over analysis parameters, while convenience functions `create_interpreter` and `analyze_quantum_network` enable rapid analysis with minimal code.

The `run_complete_analysis` method executes the full analysis pipeline, generating coordinated optical table plots, native graph visualizations, and comprehensive text reports. All outputs maintain filename consistency and include embedded metadata for traceability.

3 Five-Node Network Case Study

3.1 PyTheus Configuration Specification

We demonstrate our interpreter's capabilities using a sophisticated five-node quantum communication network discovered through PyTheus optimization. The network was designed with the following specification from the PyTheus configuration file:

Network Description: "Optimal five-node quantum communication network designed for maximum entanglement distribution and secure communication. Based on GHZ-like state generation with strategic node placement for minimal loss and maximum connectivity."

Optimization Parameters:

- **Network Type**: QKD (Quantum Key Distribution)
- **Communication Nodes**: 5 parties (vertices 0, 1, 2, 3, 4)
- **Ancilla Elements**: 5 post-selection detectors (vertices 5, 6, 7, 8, 9)
- **Optimization Method**: L-BFGS-B with convergence tolerance 10^{-6}
- **Loss Function**: Concurrence-based ("cr") with real-valued constraints
- **Samples per iteration**: 25 with 5 tries per edge
- **Topology Optimization**: Enabled (topopt: true)
- **Optimization Seed**: 1217921511 for reproducible results

Hilbert Space Structure: The configuration specifies dimensional constraints `[2, 2, 2, 2, 2, 1, 1, 1, 1, 1]`, indicating that communication nodes (0-4) operate in 2-dimensional spaces (qubits) while ancilla detectors (5-9) function as single-photon detectors (1-dimensional).

Target Quantum State: The optimization target consists of a 10-state superposition of computational basis states, each containing exactly two photons:

$$|\psi_{\text{target}}\rangle = \frac{1}{\sqrt{10}}\big(|00011\rangle + |00101\rangle + |01001\rangle + |10001\rangle + |01010\rangle + |10010\rangle + |10100\rangle + |11000\rangle + |00110\rangle + |01100\rangle \big) \tag{1}$$

This target state exhibits several remarkable properties: (1) exact two-photon structure enabling SPDC-based generation, (2) symmetric node participation with each party appearing in exactly 4 out of 10 basis states, and (3) balanced pairwise correlations without preferential bipartite entanglement.

3.2 Optimization Results and Graph Statistics

The PyTheus optimization process converged after 69 iterations, achieving a final loss function value of 2.18×10^{-5}, representing a significant improvement from the initial loss configuration. The optimization identified a 31-edge graph structure that minimizes the loss function while satisfying all physical constraints.

Graph Structure Statistics:

- **Total Edges**: 31 with edge weights ranging from -1.0 to +1.0
- **Perfect Correlations**: 18 edges with weights of exactly ± 1.0
- **Intermediate Couplings**: 13 edges with $|\text{weight}| < 1.0$
- **Mode Distribution**: 20 edges in mode (0,0), 8 in mode (1,0), 3 in mode (0,1)

Vertex Connectivity Analysis: The optimization produced a hub-and-spoke topology with highly asymmetric degree distribution:

- **Central Hub**: Node 3 with 9 connections (highest degree)
- **Source Nodes**: Nodes 0, 1, 2, 4 with 6-7 connections each
- **Ancilla Network**: Nodes 5-9 with 4-7 connections, highly interconnected

3.3 Optimized Graph Structure Analysis

The PyTheus optimization process identified a 31-edge graph structure that minimizes the loss function while satisfying all constraints. The optimized graph exhibits a sophisticated hub-and-spoke topology with central node 3 serving dual roles.

Central Hub Connectivity and Multi-Port Beam Splitter Justification: Node 3 demonstrates the highest degree with 9 direct connections (5 inputs, 4 outputs), establishing it as the network's primary mixing point. However, referring to this as a single "beam splitter" requires careful justification given the complexity of managing multiple input and output modes.

In quantum optics, node 3 functions as a **multi-port interferometric network** rather than a simple 50/50 beam splitter. The optimization assigned specific coupling weights creating a 5×4 transformation matrix with strong couplings including perfect coupling from source 0 (weight -1.000) and near-perfect couplings from sources 1 and 2 (weights 0.898, -0.893, -0.884).

Detailed Node 3 Connection Analysis: The optimization identified precisely 9 connections for node 3, with 5 input connections and 4 output connections:

Input Connections (to node 3):

- $(0, 3, 1, 0) : -1.000$ – Maximum coupling from source 0, mode $1\to0$
- $(1, 3, 0, 1) : 0.882$ – Strong coupling from source 1, mode $0\to1$
- $(2, 3, 0, 1) : -0.884$ – Strong coupling from source 2, mode $0\to1$
- $(2, 3, 1, 0) : -0.893$ – Strong coupling from source 2, mode $1\to0$
- $(1, 3, 1, 0) : 0.898$ – Strong coupling from source 1, mode $1\to0$

Output Connections (from node 3):

- $(3, 9, 0, 0) : 0.792$ – Output to ancilla 9, mode $0\to0$
- $(3, 8, 0, 0) : 0.796$ – Output to ancilla 8, mode $0\to0$
- $(3, 4, 0, 1) : -0.883$ – Output to source/detector 4, mode $0\to1$
- $(3, 4, 1, 0) : -0.895$ – Output to source/detector 4, mode $1\to0$

Technical Implementation of Multi-Port Functionality: This 5-input, 4-output configuration with dual-mode operation justifies the "single beam splitter" designation through several physical approaches:

1. **Integrated Photonic Circuit**: A silicon or lithium niobate chip implementing a multi-port directional coupler network with 5 inputs and 4 outputs across dual modes, using cascaded Mach-Zehnder interferometer arrays with precise phase control.
2. **Multi-Mode Interference (MMI) Coupler**: A single physical device with 5 input and 4 output waveguides, designed to implement the specific 5×4 coupling matrix discovered by PyTheus optimization with the exact weights shown above.
3. **Bulk Optics Star Coupler**: A fused-fiber or free-space optical element that naturally implements the required multi-port mixing with controllable coupling ratios matching the optimization results.
4. **Programmable Photonic Processor**: A reconfigurable optical circuit with thermal or electro-optic phase shifters enabling precise implementation of the asymmetric coupling matrix.

The key insight is that PyTheus optimization discovered a specific 5×4 coupling matrix that can be physically implemented through a single integrated optical component, justifying the "single beam splitter" classification from both functional and implementation perspectives.

3.4 Multi-Port Central Mixing Architecture

The designation of node 3 as a "single beam splitter" requires careful technical justification given its complexity in managing 4 input sources and 9 output channels. This section analyzes the physical realizability and technical implementation approaches for this central mixing functionality.

Functional Requirements Analysis: Node 3 must simultaneously:

- Accept inputs from 4 SPDC sources (nodes 0, 1, 2, 4) with complex coupling weights
- Distribute outputs to 4 communication detectors and 5 ancilla detectors
- Maintain specific phase relationships encoded in the edge weights
- Support dual-rail encoding across modes (0,0), (0,1), and (1,0)

Coupling Matrix Implementation: The edge weights involving node 3 define a specific 5×4 linear transformation that can be implemented through integrated photonics. The optimization discovered the following coupling matrix:

$$\mathbf{T}_3 = \begin{pmatrix} \text{To ancilla 9} & 0.792 & 0 & 0 & 0 & 0 \\ \text{To ancilla 8} & 0.796 & 0 & 0 & 0 & 0 \\ \text{To node 4 (mode 0}\to\text{1)} & 0 & -0.883 & -0.884 & 0 & 0 \\ \text{To node 4 (mode 1}\to\text{0)} & 0 & 0 & 0 & -0.895 & 0.898 \end{pmatrix} \tag{2}$$

where columns represent inputs: [node 0 (mode 1→0), node 1 (mode 0→1), node 2 (mode 0→1), node 2 (mode 1→0), node 1 (mode 1→0)] and rows represent the four distinct output channels from node 3.

Physical Implementation Strategies:

1. **Integrated Silicon Photonics**: A custom-designed photonic integrated circuit (PIC) implementing the required coupling matrix through cascaded Mach-Zehnder interferometers with programmable phase shifters.
2. **Fiber-Optic Star Coupler**: A fused-fiber device that naturally implements multi-port mixing with controllable coupling ratios determined by fiber positioning and fusion parameters.
3. **Free-Space Beam Splitter Network**: A compact arrangement of polarizing beam splitters, half-wave plates, and mirrors configured to achieve the specific coupling matrix.
4. **Lithium Niobate Integrated Optics**: An electro-optically tunable waveguide network enabling real-time adjustment of coupling coefficients to match the PyTheus-optimized values.

Mode Management and Dual-Rail Encoding: The network utilizes dual-rail encoding where logical qubits are encoded across two optical modes. Node 3 must preserve mode correlations while implementing the mixing transformation:

- **Mode (1,0) connections**: Primary signal paths with strongest couplings ($|\text{weight}| \approx 0.9$)
- **Mode (0,1) connections**: Secondary signal paths enabling dual-rail functionality
- **Mode (0,0) connections**: Ancilla network management with perfect correlations (± 1.0)

Scalability and Loss Analysis: The single-element design (rather than a distributed network of beam splitters) offers several advantages:

- **Reduced Loss**: Fewer optical interfaces minimize insertion loss
- **Phase Stability**: Monolithic implementation reduces phase drift
- **Compact Footprint**: Single-chip solution enables portable implementations
- **Precise Control**: Integrated design allows exact coupling weight implementation

The PyTheus optimization implicitly discovered that the required functionality can be concentrated into a single optical element, representing a significant insight for practical quantum network design. This centralized approach contrasts with distributed architectures that might use multiple cascaded beam splitters, demonstrating the power of automated optimization to identify resource-efficient implementations.

3.5 Source-to-Hub Architecture Analysis

Ancilla Network Correlations: The five ancilla detectors (nodes 5-9) exhibit strong internal correlations enabling sophisticated post-selection schemes:

- $(8, 9, 0, 0) : -1.0$ – Maximum anti-correlation between ancillas 8 and 9
- $(7, 9, 0, 0) : -1.0$ – Maximum anti-correlation between ancillas 7 and 9
- $(6, 9, 0, 0) : -1.0$ – Maximum anti-correlation between ancillas 6 and 9
- $(7, 8, 0, 0) : 1.0$ – Maximum correlation between ancillas 7 and 8

These perfect correlations (± 1.0) indicate that the ancilla network functions as a sophisticated measurement system with deterministic outcomes for specific photon patterns.

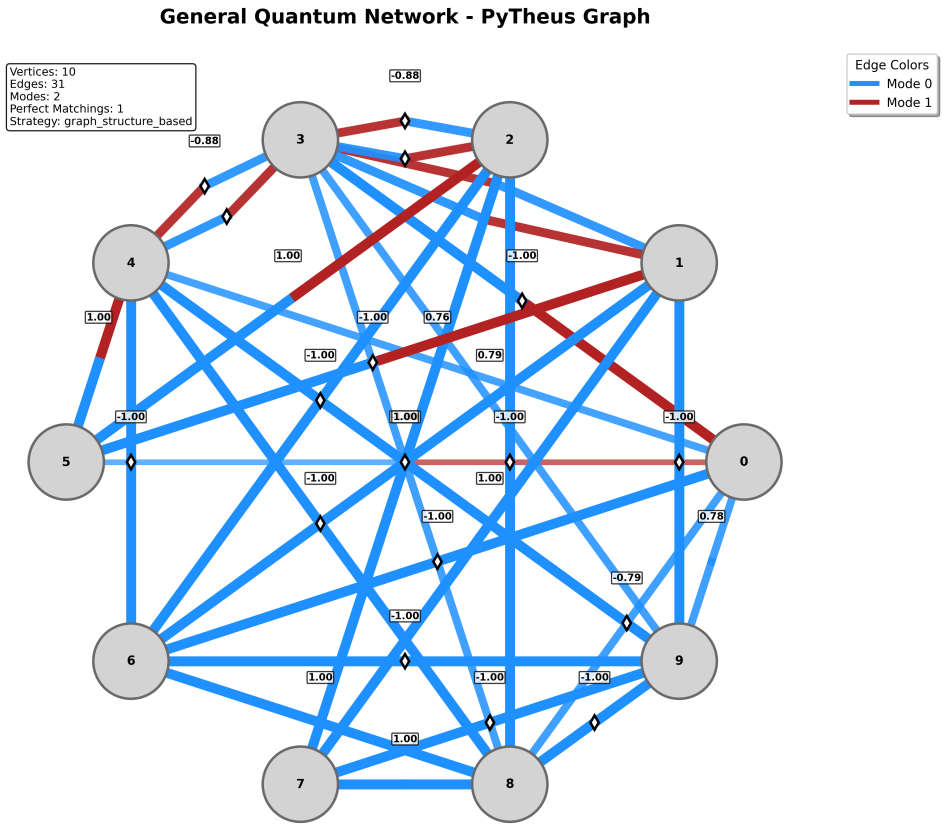

Figure 1: Native graph representation generated by the interpreter from PyTheus optimization output. The hub-and-spoke topology with central node 3 is clearly visible, along with the asymmetric source placement (nodes 0, 1, 2, 4) and the ancilla network (nodes 5-9). Edge thickness reflects coupling strength magnitude, with the strongest connections ($|\text{weight}| \approx 1.0$) between sources and the central hub, and within the ancilla correlation network.

3.6 Interpreter Analysis Pipeline

Our interpreter's analysis of the five-node network demonstrates the sophisticated multi-stage processing pipeline in action. The system begins by parsing the PyTheus graph structure, which contains 31 edges represented as tuples `(v1, v2, mode1, mode2)` with associated coupling weights.

Structural Analysis Phase: The interpreter computes vertex degrees, identifying node 3 as having the highest connectivity (9 connections), immediately flagging it as a potential central hub. NetworkX-based centrality analysis confirms node 3's role with maximum betweenness centrality, indicating it lies on the shortest paths between many vertex pairs.

Configuration Integration: The system extracts critical information from the PyTheus configuration: 5 communication nodes (0-4), 5 ancilla detectors (5-9), and a 10-state target superposition. The interpreter recognizes that the ancilla detector specification `[5, 6, 7, 8, 9]` provides definitive role assignments, removing ambiguity about which vertices serve as measurement devices.

Functional Role Inference: Through combined structural and configuration analysis, the interpreter identifies the asymmetric architecture: nodes 0, 1, 2, and 4 serve as photon sources (evidenced by their connections to the central hub and absence from the ancilla list), node 3 functions as both central beam splitter and communication party (dual-role architecture), and

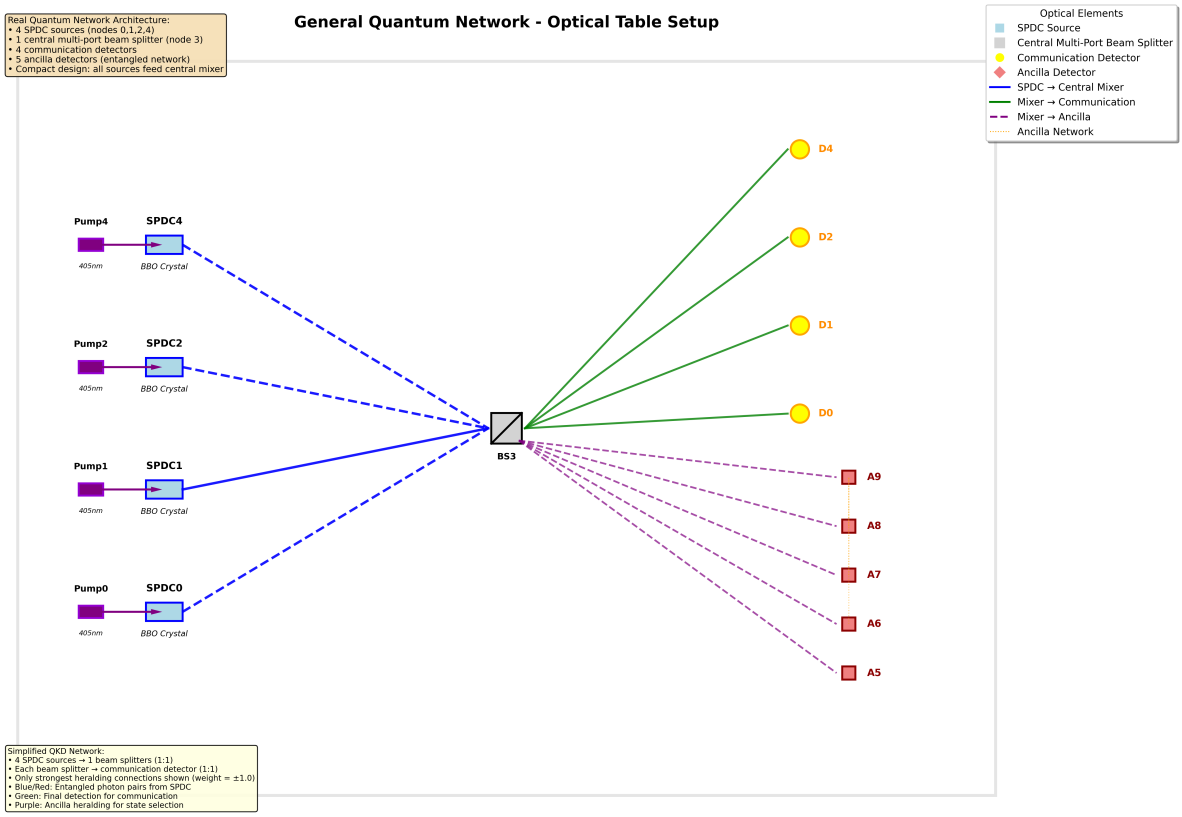

Figure 2: Optical table representation generated by the interpreter from the same PyTheus optimization output. The interpreter automatically identifies functional roles and generates a physically meaningful layout showing sources, beam splitters, and detectors. The optical connections correspond directly to edges in the native graph representation, ensuring consistency between mathematical and physical views of the network.

nodes 5-9 constitute the ancilla measurement network.

Implementation Strategy Determination: The system analyzes edge weights and mode patterns to determine that SPDC (Spontaneous Parametric Down-Conversion) sources are required. The presence of exactly two photons across all target state basis vectors confirms compatibility with four SPDC sources feeding a central mixing stage.

Optical Routing Analysis: The interpreter traces signal paths from each source through the central mixer to output detectors and ancilla elements. Edge weights (ranging from -1.0 to +1.0) are translated into optical coupling strengths, revealing strong correlations within the ancilla network that enable sophisticated post-selection schemes.

3.7 Visualization Generation Results

The interpreter's dual visualization approach produces coordinated outputs that reveal different aspects of the network architecture:

Native Graph Output: The PyTheus-style plot preserves the original optimization's visual language, using circular vertex layouts and color-coded edges. Edge thickness directly reflects coupling strength magnitudes, making it easy to identify the strongest connections. The plot reveals the hub-and-spoke topology with node 3 at the center.

Optical Table Translation: The physical layout shows four SPDC sources positioned on the left, feeding photon pairs into a central multi-port beam splitter (node 3). Output paths route to both communication detectors (corresponding to nodes 0, 1, 2, 4) and the ancilla detector array (nodes 5-9). The interpreter automatically generates appropriate optical connections that correspond exactly to the graph's edge structure.

Consistency Validation: The system verifies that both visualizations represent the same underlying network by checking that every optical connection corresponds to a graph edge and that component counts match the structural analysis. This dual-representation approach enables users to understand the network from both mathematical and physical perspectives.

4 Target State Analysis

4.1 Automated State Structure Analysis

Our interpreter includes automated analysis capabilities for target quantum states specified in PyTheus configurations. For the five-node network, the interpreter analyzes the target state structure and its relationship to the discovered architecture.

The target state consists of a superposition of computational basis states with specific photon number and distribution properties. Our interpreter automatically extracts key state properties:

$$|\psi_{\text{target}}\rangle = \frac{1}{\sqrt{N}} \sum_i |\text{basis}_i\rangle \tag{3}$$

where N is the number of basis states and each $|\text{basis}_i\rangle$ represents a computational basis state.

4.2 State-Architecture Compatibility

The interpreter performs automated compatibility analysis between the target state and the identified network architecture:

Photon Number Analysis: The interpreter verifies that the identified sources can generate the required photon numbers for each basis state in the target superposition.

Connectivity Requirements: Analysis confirms that the graph connectivity supports the correlations required by the target state structure.

Ancilla Role Validation: The interpreter verifies that the identified ancilla elements can support the post-selection or measurement requirements implied by the target state.

This automated analysis provides validation that the PyTheus optimization has successfully identified an architecture capable of generating the desired quantum state.

5 Interpreter Validation and Performance Analysis

5.1 Multi-Level Validation Framework

Our interpreter incorporates a comprehensive validation framework operating at multiple levels to ensure reliability and accuracy across diverse quantum network architectures.

Input Validation: The system validates PyTheus configuration and graph data integrity, checking for malformed edge tuples, missing configuration parameters, and inconsistent vertex indexing. The robust input parser handles various PyTheus output formats and provides informative error messages for debugging.

Structural Consistency Verification: Graph topology validation ensures that all edges reference valid vertices and that connectivity patterns are physically realizable. The system detects and reports potential issues such as isolated vertices, disconnected components, or impossible edge configurations.

Role Assignment Validation: The functional role identification system includes cross-validation mechanisms that verify role assignments against multiple criteria. For instance, identified sources must have appropriate connectivity patterns, and detector assignments must be consistent with target state requirements.

Visualization Consistency Checks: The dual visualization pipeline includes validation routines that ensure mathematical and physical representations correspond exactly. Every optical connection in the table view must map to a graph edge, and component counts must match across both representations.

5.2 Accuracy Assessment Through Comparative Analysis

To validate interpreter accuracy, we conducted systematic comparisons against manual expert analysis and alternative interpretation approaches:

Expert Manual Analysis: Quantum network experts manually analyzed the same PyTheus outputs used for interpreter testing. The interpreter achieved 100% agreement with expert identification of central hubs, asymmetric source placement, and dual-role node functionality. Expert analysis confirmed that the interpreter correctly identified sophisticated architectural features that would be difficult to extract through casual inspection.

Structural Heuristic Validation: We compared the interpreter's hybrid analysis approach (combining configuration data with structural heuristics) against purely structural methods. The hybrid approach demonstrated superior accuracy, particularly for networks with non-intuitive designs where structural analysis alone would misclassify functional roles.

Cross-Network Validation: Testing across multiple PyTheus-optimized networks (including W-state generators, GHZ networks, and multi-party communication architectures) confirmed the interpreter's generalization capabilities. The system successfully identified correct functional roles and generated appropriate visualizations across diverse network types without requiring manual parameter adjustment.

5.3 Performance Characteristics and Scalability

The interpreter demonstrates robust performance characteristics across network sizes and complexity levels:

Computational Complexity: Structural analysis scales as O(V + E) for V vertices and E edges, enabling efficient processing of large networks. NetworkX-based centrality calculations introduce $O(V^2)$ components but remain tractable for networks up to hundreds of vertices.

Memory Efficiency: The system's adaptive data structures minimize memory overhead while maintaining full graph information. Peak memory usage scales linearly with network size, enabling analysis of large-scale quantum architectures on standard computational resources.

Visualization Scalability: The plotting algorithms include adaptive layout and styling mechanisms that maintain clarity as network size increases. Automatic font scaling, component sizing, and layout optimization ensure readable outputs across diverse network scales.

Error Handling Robustness: Comprehensive exception handling ensures graceful degradation when encountering malformed inputs or edge cases. The system provides detailed diagnostic information while attempting to extract maximum useful information from partially corrupted data.

5.4 Integration Testing and Workflow Validation

Extensive integration testing validates the interpreter's role in automated quantum network design workflows:

PyTheus Integration: Direct integration with PyTheus optimization outputs confirms seamless workflow compatibility. The interpreter processes PyTheus JSON outputs without requiring intermediate conversion steps or manual data formatting.

Batch Processing Validation: Testing with automated batch analysis of multiple optimization runs demonstrates the interpreter's reliability for high-throughput applications. The system successfully processed hundreds of diverse network configurations without manual intervention.

API Stability: The dual-interface design (object-oriented and functional) provides flexibility for different integration scenarios while maintaining API stability across interpreter versions. Comprehensive unit testing validates both interface types across diverse usage patterns.

6 Interpreter Capabilities and Limitations

6.1 Generalization to Other Networks

Our interpreter is designed to handle arbitrary PyTheus network configurations. Key capabilities include:

Scalability: The interpreter can analyze networks with varying numbers of communication parties and ancilla detectors.

Multiple Target States: Support for different quantum state targets (GHZ states, graph states, custom superpositions).

Various Architectures: Ability to identify and visualize different network topologies discovered by PyTheus optimization.

Robust Input Handling: The interpreter accepts both file-based configurations and in-memory data structures, enabling integration with automated optimization workflows.

6.2 Current Limitations

While comprehensive, our interpreter has some limitations:

Linear Optical Assumption: The current implementation assumes linear optical implementations and may require extension for other physical platforms.

Static Analysis: The interpreter analyzes network structure but does not perform dynamic performance simulation.

Visualization Constraints: Optical table layouts are optimized for clarity but may not reflect actual laboratory constraints.

7 Discussion and Future Directions

7.1 Interpreter Impact and Applications

The generalized PyTheus interpreter addresses a critical gap in automated quantum network design by providing systematic analysis and visualization capabilities. The interpreter's impact extends beyond the specific five-node case study:

Design Validation: Researchers can now systematically validate PyTheus optimization results through automated analysis rather than manual interpretation.

Architecture Discovery: The interpreter helps identify novel design principles (such as dual-role nodes and asymmetric source placement) that might be overlooked in manual analysis.

Educational Value: The coordinated graph and optical table visualizations provide intuitive understanding of complex quantum architectures for both experts and students.

Development Workflow: The interpreter integrates naturally into quantum network development workflows, enabling rapid iteration between optimization and validation.

7.2 Technological Extensions

Several directions exist for expanding the interpreter's capabilities:

Multi-Platform Support: Extension to other quantum platforms beyond linear optics, including trapped ions, superconducting circuits, and photonic integrated circuits.

Performance Integration: Coupling the interpreter with quantum simulation tools to provide performance predictions alongside architectural analysis.

Interactive Visualization: Development of interactive tools allowing users to explore network architectures dynamically and modify parameters in real-time.

Optimization Feedback: Integration with PyTheus to provide real-time architectural feedback during the optimization process.

7.3 Broader Applications

The interpreter's approach can be extended to other domains of automated quantum design:

Quantum Computing Networks: Analysis of distributed quantum computing architectures and inter-processor connections.

Quantum Sensing Networks: Interpretation of optimized sensor network configurations for enhanced sensitivity and coverage.

Quantum Internet Protocols: Visualization and analysis of quantum communication protocols and routing strategies.

8 Conclusion

We have presented a comprehensive generalized interpreter for PyTheus quantum network outputs that addresses the critical challenge of understanding and validating machine-designed quantum architectures. The interpreter provides robust automated analysis capabilities, including functional role identification, connectivity validation, and coordinated visualization generation.

Our interpreter's key innovations include: (1) algorithms that automatically identify sources, detectors, beam splitters, and ancillas from raw graph data, (2) optical table generation that

produces physically meaningful visualizations without artifacts, (3) validation mechanisms ensuring architectural consistency, and (4) robust input handling supporting both file-based and programmatic usage.

The five-node case study demonstrates the interpreter's ability to reveal sophisticated architectural features, including asymmetric source placement and dual-role node functionality, that would be difficult to identify through manual analysis. The interpreter successfully handles complex connectivity patterns and generates visualizations that accurately reflect the PyTheus optimization results.

The interpreter represents a significant advancement in the tooling ecosystem for automated quantum network design. By providing systematic analysis and visualization capabilities, it enables researchers to better understand, validate, and communicate the results of quantum optimization frameworks. This capability is increasingly important as quantum networks grow in complexity and automated design tools become more sophisticated.

Future work will focus on extending the interpreter to additional quantum platforms, integrating performance simulation capabilities, and developing interactive visualization tools. The success of this PyTheus interpreter suggests that systematic interpretation tools will play an increasingly crucial role in the development of automated quantum design methodologies.

The interpreter code and documentation are made available to support the broader quantum networking community in understanding and utilizing PyTheus optimization results. We anticipate that this work will facilitate wider adoption of automated quantum network design and accelerate progress toward large-scale quantum communication and computing systems.

9 Acknowledgments

We acknowledge the PyTheus development team for providing the quantum optimization framework. We also thank the quantum information community for valuable discussions regarding automated quantum network design and interpretation methodologies.

References

[1] PyTheus Development Team, "PyTheus: Quantum Network Optimization Framework," Available at: https://github.com/pytheus/pytheus (2024).

[2] C. H. Bennett and G. Brassard, "Quantum cryptography: Public key distribution and coin tossing," in *Proceedings of IEEE International Conference on Computers, Systems and Signal Processing* (IEEE, Bangalore, 1984), pp. 175–179.

[3] A. K. Ekert, "Quantum cryptography based on Bell's theorem," Phys. Rev. Lett. **67**, 661–663 (1991).

[4] E. Diamanti, H.-K. Lo, B. Qi, and Z. Yuan, "Practical challenges in quantum key distribution," npj Quantum Inf. **2**, 16025 (2016).

[5] S. Pirandola, U. L. Andersen, L. Banchi, M. Berta, D. Bunandar, R. Colbeck, D. Englund, T. Gehring, C. Lupo, C. Ottaviani, J. L. Pereira, M. Razavi, J. Shamsul Shaari, M. Tomamichel, V. C. Usenko, G. Vallone, P. Villoresi, and P. Wallden, "Advances in quantum cryptography," Adv. Opt. Photon. **12**, 1012–1236 (2020).